Modal Testing and Analysis of High-rise Laminated Timber Building

Qiyun Xu,[a] Hongyan Zou,[c] Zheng Wang,[a,*] Yuhang He,[b] Liang Qi,[c] and Jun Wang [d]

To enhance the design and research work on dynamic characteristics of high-rise laminated timber buildings, this paper carried out a modal analysis study on one of the largest laminated timber buildings in China. The finite element calculating modal analysis was carried out using SAP2000 software, and the experimental modal analysis of the building was carried out *via* environmental excitation. The calculating modal results and the experimental modal results showed good agreement. The calculating modal frequency values were generally lower than the experimental modal frequency values. The natural frequencies obtained by the two methods appeared in the Y-direction first-order bending mode and had values of 2.03 and 2.5 Hz, respectively. The corresponding frequencies of the first-order torsional mode were 2.82 and 3.25 Hz, respectively. The distribution of the CLT core tube along the length direction of the building has an impact on the vibration mode. The six-story part shows the second-order bending form, while the four-story section only shows the first-order bending form. The above work provides a case study and reference for the simulation and modal analysis of high-rise laminated timber buildings, demonstrating the critical role of the core tube structure in such wooden buildings. This insight contributes to a better understanding of structural performance and design considerations in similar projects.

DOI: 10.15376/biores.19.4.9616-9630

Keywords: Laminated timber; Natural frequency; Dynamic characteristics; Calculating modal; Experimental modal

*Contact information: a: College of Materials Science and Engineering, Nanjing Forestry University, Nanjing, Jiangsu, China; b: College of Civil Engineering, Southeast University, Nanjing, Jiangsu, China; c: College of Mechanical and Electronic Engineering, Nanjing Forestry University, Nanjing, Jiangsu, China; d: College of Information Science and Technology, Nanjing Forestry University, Nanjing, Jiangsu, China; *Corresponding author: wangzheng63258@163.com*

INTRODUCTION

As a type of building material, glulam (glued-laminated timber) has been widely used in the construction industry and is favored for its unique advantages. Glulam features high strength, good stability, and moisture resistance. However, its drawbacks include a higher cost and the potential for reduced performance in extreme environments due to the effects of the adhesive. Nevertheless, glulam not only enhances the stability and durability of the wood, but also improves its mechanical properties, making it ideal for large structures and complex designs. The glulam structure has been applied to emporiums, gymnasiums, schools, restaurants, libraries, and other large public buildings (Sueyoshi 2008; Hayashi and Miyatake 2015), such as the Tacoma Dome gymnasium (USA) and the Bullitt Center in Seattle (USA). In China, glulam buildings have accounted for 16% of the whole wood buildings.

Modern wooden structure buildings are showing a rapid development trend, and significant progress has been made in research on building materials, component connections, fire resistance, and anti-corrosion capabilities (Jiang *et al.* 2022; Quintero *et al.* 2022; Wang and Ghanem 2023). The traditional structural design and structural analysis theory mainly considers the strength, stiffness, and stability of the structure. However, in most cases, the results that cause structural failure are most affected by dynamic loads. Therefore, in addition to obtaining the static characteristics of the building structure, scholars also focus on the dynamic characteristics of the building structure under the action of dynamic loads. Reynolds *et al.* (2015) took a seven-story cross-laminated timber (CLT) wood structure building as an object, measured the dynamic characteristics of the building at two construction stages on site using the environmental excitation method, and extracted the modal parameters of the structure from the acceleration response using random subtraction method and Ibrahim time-domain method. Hafeez *et al.* (2019) conducted environmental excitation tests on 41 light wood structures in different regions of Canada and obtained the dynamic characteristic parameters of the buildings through finite element numerical simulation. Zhang *et al.* (2021) developed twenty-two three-dimensional finite element models with different connection combinations to study the effects of fasteners between CLT plates, and shear stiffness on the dynamic characteristics and seismic performance of CLT buildings. These studies have conducted dynamic characteristics research on both heavy and light wooden structures, as well as on wooden structure building nodes, which have high reference values for improving the level of research and design on dynamic characteristics of wooden structure buildings.

When previous researchers conducted research on the dynamic characteristics of building structures, they usually took the modal shapes of the building as the starting point. Modal analysis is a principal technique utilized to investigate the dynamic properties of structures. Through modal analysis, the natural vibration characteristics of the structure can be obtained. For large wooden structures, the energy generated by human excitation is difficult to transmit within the structure, so it is necessary to use environmental excitation methods to analyze the building structure. At present, research projects carried out on the dynamic characteristics of multi-story laminated wood structures often are excessively simplistic, lacking research results that combine experimental modal analysis with experimental modal analysis. Most of them only obtain the experimental modal shapes and modal parameters of the building structure through testing. However, a single experimental modal analysis will mask the influence of factors, such as the structural characteristics of the building itself and material defects. The theoretical basis is often insufficient, which is not conducive to researchers' and designers' understanding and mastery of the local and overall aspects of the building. At the same time, the characteristic values of the nine independent elastic constants of the materials used by a large number of researchers in the finite element calculation of wood structure buildings usually refers to the existing literature, rather than the measured data, so that the simulation results are not supported by data and their reliability needs to be verified. Therefore, this work involved a modal analysis on a large glulam structure building in China. Through the calculating modal analysis and experimental modal analysis of the building, the characteristic parameters, such as vibration mode and natural frequency of the structure are expected to be mastered. The finite element simulation was carried out with nine independent elastic constants of the material, which were measured accurately. The modal and frequency values of the experimental modal were guided by the calculated modal results, and the accuracy of the calculated modal results was verified by the experimental modal results. The two results

were analyzed and discussed. This work has a high value for engineering projects and practical significance for optimizing the design of large timber structures, including glulam buildings, as well as engineering inspection and research on their dynamic characteristics.

CALCULATING MODAL ANALYSIS

Research Object

The research object is the R&D center building of Shandong Dingchi Wood Industry Group, located in Penglai District, Yantai City, Shandong Province, with a length of 66.9 m, a width of 17.4 m, a maximum height of 24.7 m, and a total construction area of 4778.5 m^2. The building is a glulam frame shear wall structure. The main structure is made of glulam, and the lamination is SPF (Spruce-pine-fir). The stairwell walls are made of CLT shear walls. The remaining walls are mainly light wood shear walls. Building structural materials were produced in Canada and processed by Shandong Dingchi Wood Industry Group Co., LTD. The R&D center building is mainly composed of a beam-column frame system consisting of one type of glued timber column and four types of glued timber beams. The first and sixth floors of the building are 4.15 m and 4.7 m high, respectively, and the height of the other floors is 3.4 m. The effective length of each layer of light wood shear wall is the same, and the edge wall bone column is SPF specification material. The building is shown in Fig. 1.

Fig. 1. Shandong Dingchi Wood Industry Group R&D center building

Test and Results of Building Structure Material Parameters

More than 85% of the structural materials of the R&D center building are spruce-pine-fir (SPF) species. In the macro-analysis of wood structure buildings, it is assumed that wood is a continuous and uniform orthotropic material with flat texture and no growth defects and has 9 independent elastic constants, namely 3 elastic moduli, 3 shear moduli, and 3 Poisson's ratio (Wang *et al.* 2014; Wang *et al.* 2022).

The wood has three main directions and three sections, and the three main directions are the direction of grain, radial, and chord, respectively, which are represented by the letters L, R, and T. The three sections are radial section (LR or RL), tangential section (LT or TL), and cross-section (RT or TR). The nine independent elastic constants of SPF timber are expressed as 3 elastic moduli E_L, E_T, and E_R, 3 shear moduli G_{LR}, G_{LT}, and G_{RT}, and 3 Poisson ratios μ_{LR}, μ_{LT}, μ_{RT} or μ_{TR}, respectively.

In this paper, a series of SPF specifications provided by Shandong Dingchi Wood Industry were tested. Through the CRAS dynamic signal acquisition and analysis system, the free board transient excitation method (Wang *et al.* 2015; Gao *et al.* 2016; Wang *et al.* 2018) was used to measure the elastic modulus E and shear modulus G of all sides upward of the SPF specimen, and the cantilever board transient excitation method (Wang *et al.* 2016) was used to obtain the Poisson ratio μ of all sides upward of SPF timber. The specifications and quantities of test specimens used are shown in Table 1. The average air-dry density of SPF specimens was 420 kg/m^3, and the moisture content was 7 to 10%. The symmetrical four-point bending method and the asymmetric four-point bending method (Wang *et al.* 2019, 2023) of beam specimens were also used to verify the accuracy of dynamic test results. The test results of SPF specimens are shown in Table 2, and the dynamic and static errors of the nine elastic constants did not exceed 10%. Therefore, the results of elastic modulus, shear modulus, and Poisson's ratio of SPF timbers tested by dynamic free plate and cantilever plate in this study were judged to be reliable and were applied to the numerical analysis of finite element calculating modal analysis.

Table 1. Specifications and Quantity Table of Board and Beam Specimens

Specimen	Dimension (mm)	Quantity (Block)
LR board	Length 300, width 50, thickness 8	11
LT board	Length 300, width 50, thickness 8	11
TR board	Length 233, width 35, thickness 7	11
RT board	Length 233, width 35, thickness 7	11
LT board	Length 240, width 20, thickness 20	11
LR board	Length 240, width 20, thickness 20	11

Table 2. Dynamic and Static Test Results of SPF Specimen

Elastic Constant	Dynamic Result	Static Result	Absolute Error (Relative Error)
E_L	12367 MPa	13330 MPa	-963 MPa (-7.2%)
E_T	365 MPa	——	——
E_R	689 MPa	——	——
G_{LT}	594 MPa	598 MPa	-4 MPa (-0.7%)
G_{LR}	653 MPa	683 MPa	-30 MPa (-4.4%)
G_{TR}	108 MPa	——	——
μ_{LT}	0.44	0.40	0.04 (10.0%)
μ_{LR}	0.34	0.33	0.01 (3.0%)
μ_{RT}	0.61	——	——
* Note: "——" means undetectable			

Finite Element Simplification of the Building Structure

By utilizing the elastic modulus and thickness of the laminated wood, the elastic modulus of glulam beams and columns can be calculated based on the sum of the torque generated by the normal stress on the cross-section to the neutral layer as the bending moment received. The laminates of the glulam used in this study are of equal thickness and have the same assemble patterns. According to the above relationship, the elastic modulus

of glulam is approximately equal to that of laminates. Furthermore, according to the analysis of symmetrically laminated glulam in ASTM D3737-09 (2009), the elastic modulus of the glulam used in this building is also approximately the elastic modulus of the laminated board.

For the analysis of the overall dynamic characteristics of the building, the CLT wall is simulated with orthotropic thin-shell elements. The balsa shear wall is modeled as a diagonal spring element with the ends hinged to the beams and columns, taking into account only its resistance to lateral forces. Figure 2 illustrates the simplified structure.

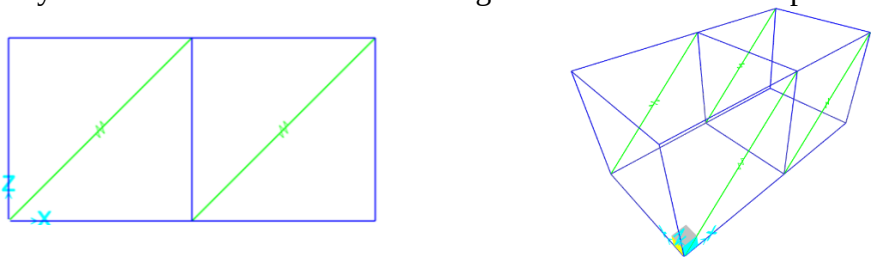

Fig. 2. Constructing a simplified model

This paper refers to the calculation method of lateral stiffness of balsa wood shear wall involved in the technical regulations for light wood structure buildings (DG/T J08-2059 2009), and considers the bending deformation of wall bone columns, shear deformation of cladding panels, and vertical deformation of the bottom of the shear wall, and calculates the equivalent horizontal lateral stiffness *K'* per unit length of single-sided cladding shear wall with Eq. 1, Eq. 2, and Eq. 3:

$$k_d = \frac{1}{\frac{2h_{\mathrm{w}}^3}{3EAL_{\mathrm{W}}} + \frac{h_{\mathrm{w}}}{1000G_{\mathrm{a}}} + \frac{h_{\mathrm{w}}}{L_{\mathrm{w}}} \cdot \frac{d_{\mathrm{n}}}{f_{\mathrm{vd}}}} \quad (1)$$

$$K = \sum \gamma_1\gamma_2\gamma_3 \cdot k_{\mathrm{d}} \cdot L_{\mathrm{w}} \quad (2)$$

$$K' = \frac{K}{|\cos\theta|} \quad (3)$$

In Eq. 1, f_{vd} is the shear strength of the unit length shear wall (kN/m); h_w is the height of the wall limb of the monolithic shear wall (mm); L_w is the length of the shear wall limb parallel to the load direction (m); A is the cross-sectional area of the wall bone column at the end of the shear wall (mm^2); E is the elastic modulus of the wall bone column at the edge of the shear wall (N/mm^2); G_a is the equivalent shear stiffness of wood-based structural panels (kN/mm); dn is the vertical deformation at the bottom of one side of the shear wall when the shear capacity f_{vd} is reached (mm); and k_d is the horizontal lateral stiffness of the unit length of the shear wall (kN/mm/m). In Eq. 2, L_w is the length of the shear wall limb parallel to the direction of load (m); γ_1 is the adjustment factor for the use environment; γ_2 is the adjustment coefficient of shear wall height-to-width ratio; γ_3 is the stiffness adjustment coefficient; K is the horizontal lateral stiffness (kN/mm/m); and $\cos\theta$ is the cosine of the angle of the spring element to the horizontal plane.

The effective lengths of the light wood shear wall are the same, and the edge studs are all made of SPF specification materials, and their elastic modulus along grain adopts the test data E_L in Table 2. The experimental data f_{vd} = 7.48 kN/m was obtained from Enchun Zhu *et al.* (2010) of Harbin Institute of Technology as the unit length shear strength

of shear walls. The unit length horizontal lateral stiffness of all shear walls in the building and the equivalent spring element stiffness were calculated according to the above equations and applied to the finite element calculation.

Main Steps of Finite Element Model Establishment

Two orthotropic materials, glulam and CLT, were added into SAP2000 software, and the elastic modulus, shear modulus, and Poisson ratio of the measured glulam and CLT materials in Table 2 were recorded in the software. SAP2000 is a powerful structural analysis and design software that supports both linear and nonlinear analysis. It features an intuitive user interface that allows users to easily create and modify models, while integrating various international design codes. The version used in this article was V18.2, which operates on a 64-bit Windows operating system. Glulam beams, and columns are defined as frame sections, while floors and CLT walls are defined as shell sections. The light wood shear wall is defined as an equivalent spring element and the equivalent stiffness value of the light wood shear wall obtained according to Eq. 3 is used as its stiffness coefficient.

According to the structural layout of the building, the whole glulam structure building was modeled by each layer. The support type of the glulam structure building was rigid-pinned (Polastri *et al.* 2019), the beam-and-column nodes were pinned and the CLT wall was holed to simulate the doors and windows. The overall building model is shown in Fig. 3. The CLT wall was divided into cell grids, and all CLT shell cells were selected according to the surface section properties. The nodes were selected where the floors were located and the nodes restraint type were specified as a diaphragm. Finally, dead load was added and modal analysis was carried out under modal conditions.

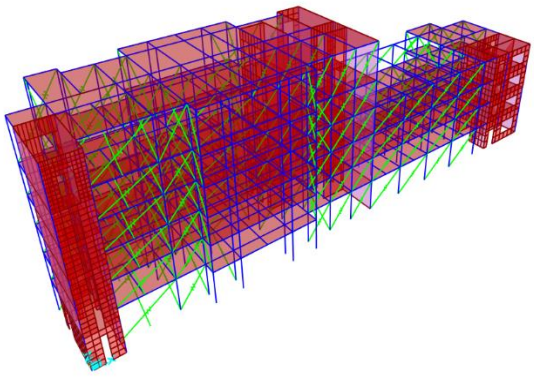

Fig. 3. 3D view of the building as a whole

EXPERIMENTAL MODAL ANALYSIS

To obtain the actual dynamic characteristics of the six-story laminated timber building in this study and verify the accuracy of the structural modal analysis, the experimental modal analysis was carried out on the R&D Center building of Shandong Dingchi Wood Industry Group (Fig. 1). The first two-order bending modal and torsional modal in the X and Y directions (Building length direction is X-direction, building width

direction is Y-direction, building height direction is Z-direction) and their corresponding frequency values were obtained.

Principle of Modal Testing Based on Environmental Excitation

The excitation methods of experimental modal analysis were mainly divided into transient excitation, steady excitation, and environmental excitation. Given the properties and effects of transient excitation and steady-state excitation, it is more reasonable and effective to apply the environmental excitation method to the modal testing of multi-story laminated timber buildings. The external environment, such as ground pulsation, wind load, and traffic load, is used to stimulate the building to vibrate, and the response signals were collected by an accelerometer or velocity meter and processed to obtain its dynamic characteristic parameters. Experimental modal analysis based on environmental excitation cannot establish a strict dynamic model because the input of the system and the transfer functions of the system are not available. Given the premise that the structural vibration system, which possesses n degrees of freedom, is stimulated by uniform white noise, the frequency response function of the input white noise on *n* degrees of freedom is:

$$\{H_1(\omega),\ H_2(\omega),\ \cdots,\ H_n(\omega)\} \tag{4}$$

This expression specifies either a column or a row in the system's mode matrix. The frequency response function for the i and j degrees of freedom when subjected to stochastic excitation can be denoted by Eq. 5:

$$H_i(\omega) = \frac{X_i \cdot \bar{F}}{F \cdot \bar{F}} = \frac{G_{x_i f}}{G_{ff}} \tag{5}$$

$$H_j(\omega) = \frac{X_j \cdot \bar{F}}{F \cdot \bar{F}} = \frac{G_{x_j f}}{G_{ff}} \tag{6}$$

In Eqs. 5 and 6, F is a spectrum, and $\bar{F}$ is its conjugate. Because the input force signal cannot be measured, to identify the vibration mode under natural environment excitation, the vibration X_i of the first reference degree of freedom *i* is replaced by F of Eq. 5 and Eq. 6, and the transfer function of the *j* degree of freedom to the *i* degree of freedom is defined as:

$$T_{ji}(\omega) = \frac{X_j \cdot \bar{X}_\iota}{X_i \cdot \bar{X}_\iota} = \frac{G_{ji}}{G_{ii}} = \frac{H_j(\omega)}{H_i(\omega)} \tag{7}$$

This transfer function is also known as the Operational Deformation State Frequency Response Function (ODS FRF). Its amplitude is,

$$\varphi_j = \left|T_{ji}(\omega_k)\right| = \sqrt{G_{jj}(\omega_k) \Big/ G_{ii}(\omega_k)}\ (j = 1,2,\ \cdots,\ n) \tag{8}$$

where φ_j = (j=1, 2, ..., n) forms the mode vector. T_{ji} is the phase difference between X_j and X_i. The modal frequency of each order under environmental excitation is the peak point frequency ω_k on the amplitude-frequency curve of the origin transfer function $T_{ji}(\omega)$, which is selected on the total average curve of the vibration power spectrum set of all measurement points.

Test Instrument and Setup

In this experiment, four 941B vibration pickups (56 mm × 56 mm × 77 mm, weight 0.75 kg) and four SYV50-3-1 cables produced by Shanghai Qiyue High-Temperature Cable Co., Ltd. were used to collect signals. The collected vibration signals were processed and fitted by vibration and dynamic signal acquisition analysis system (including modal analysis instrument and software MaCras, instrument and software developed by Nanjing Anzheng Software Engineering Co., Ltd.) and computer.

The MaCras intermediate frequency response function test excitation method was set to environmental excitation, and the number of collector channels was set to 4 channels (respectively collected as reference points X and Y signals and moving points X and Y signals). The analysis frequency was 50 Hz and the FFT block length was 1024.

Main Steps of Experimental Modal Testing

To preliminarily estimate the range of the building's natural frequency and determine the parameter settings in modal analysis software, preliminary experiments were conducted based on the calculating modal results. Because the vibration of buildings is similar to that of vertical cantilever beams, a simple model of vertical cantilever beams was established through MaCras, and the natural frequency of Y-direction was determined within 10 Hz through environmental excitation. The calculating modal frequency also satisfied the range. To eliminate the interference of high-frequency background noise, the analysis frequency range was set within 50 Hz. Due to the low natural frequency of high-rise buildings, it is not appropriate to use accelerometers suitable for obtaining medium to high frequencies. Therefore, in the overall test, the accelerometer gear of the vibration pickup will be adjusted to the speed gear for testing.

In addition, to avoid interference from human movement on the collected signal, the whole experimental modal test was carried out during non-working time at night. According to the actual size of the multi-story laminated timber structure, the model was built in MaCras software. The exterior walls of the building were meshed and test points were arranged on the ground of each floor. The test model is shown in Fig. 4.

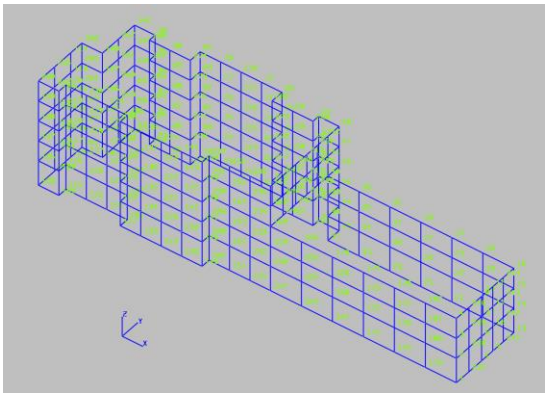

Fig. 4. Framework test model

The total number of geometric nodes in the test model was 292, among which 72 points in the first layer were model constraint points that were not involved in the test. To obtain a clearer vibration pattern, point No. 72 on the 6th floor of the building was selected as the reference point for this test, and the remaining 220 test points were tested as moving points. The X and Y direction velometers of the reference point were placed at point 72,

and the X and Y direction velometers of the moving points were placed in the remaining 220 test points for vibration pickup. The velometers at the reference points and the moving points were facing the same direction. After preliminary parameter estimation, curve fitting, modal normalization, and other steps, the modal shape was obtained. Figure 5 shows the environmental incentive test site at point 244.

(a) X and Y velometers for reference point **(b)** X and Y velometers for moving points

Fig. 5. Environmental incentive test at point No. 244

RESULTS AND DISCUSSION

Results and Discussion of Calculating Modal

The calculating modal shapes and frequency values of each order of the building are shown in Fig. 6. In Fig. 6(a), the Y-direction first-order bending amplitude of the six-story part (the tested building is of asymmetric construction, with the highest part having six floors, which is referred to as the six-story part in this article) is larger than that of the four-story part. This is because the building itself is not symmetrical and there is a height difference in the direction of its length. In addition, the amplitude of vibration modes at different positions of the six-story part is inconsistent. The CLT wall in the middle of the building has a smaller amplitude than the stairwell at the end. This is because the whole CLT wall separates the four-story part from the six-story part, and its rigidity is relatively large, which limits its Y-direction first-order bending amplitude.

In Fig. 6 (a) (b), there is a certain overlap between the Y-direction and X-direction bending modal shapes, because the CLT wall arranged in the Y-direction is more than that in the X-direction, which weakens the stiffness advantage provided by the glulam frame and the light wood shear wall in the X-direction, narrowing the first-order bending frequency of the X and Y-direction. The difference between the two is only 5.1%. In the X-direction first-order bending modal analysis shown in Fig. 6 (b), the amplitude of the six-story part is also larger than that of the four-story part. In Fig. 6 (e) (d), the six-story part has an obvious second-order bending mode, while the four-story part only has a first-order bending mode, which is caused by the large height difference between different parts of the building. The higher the number of building floors, the more easily the high-order modes will appear. In Fig. 6 (c), the center of the torsional mode is not located in the geometric center of the building but shifts toward the middle of the six-story part of the building. This is because the rigidity of the two CLT core tubes in this area is relatively large, and it is easy to form a torsional center between the two core tubes when torsional vibration occurs.

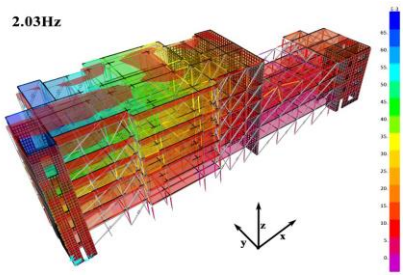

(a) First-order bending modal in Y-direction

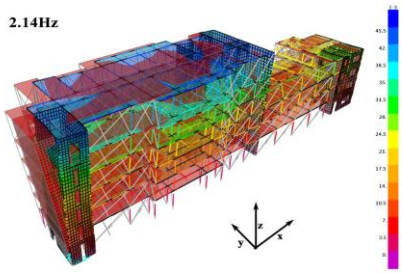

(b) First-order bending modal in X-direction

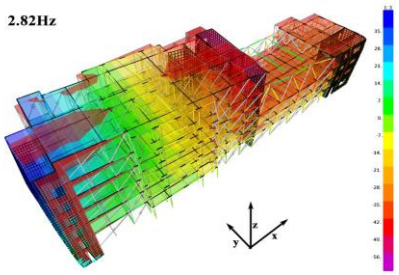

(c) First-order torsional modal shape

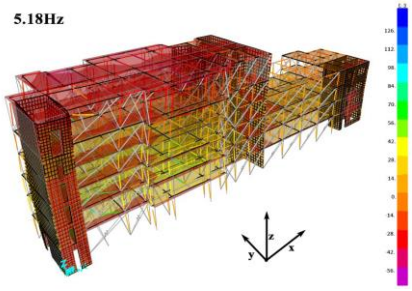

(d) Second-order bending modal in Y-direction

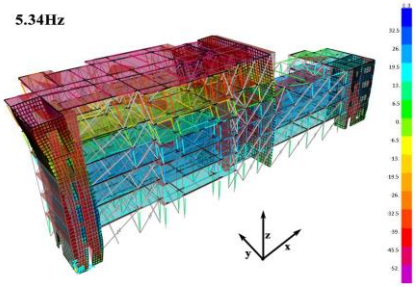

(e) A second-order bending modal in X-direction

Fig. 6. Calculating modal shapes

According to the frequency results of the calculating modal, it can be seen that the bending amplitude in the Y-direction is the smallest, indicating that the multi-story laminated timber structure is more prone to damage under the action of Y-direction bending. The first-order bending frequencies in the X and Y directions are both higher than the first-order torsion frequencies, indicating that the building is more prone to bending failure than torsion. This is because the three CLT core tubes of the building are distributed at both ends and in the middle of the length direction of the building, which plays a role in strengthening the local stiffness, thus making it difficult for the building to undergo torsion deformation.

Experimental Modal Results and Discussion of Experimental Modal

The modal test preferably obtained first-order bending, second-order bending, and first-order torsional vibration modal shapes. Among them, the first-order bending frequency in the X-direction was 2.625 Hz, the second-order bending frequency in the X-direction was 6.25 Hz, the first-order bending frequency in the Y-direction was 2.5 Hz, and the first-order torsion frequency in the X-direction was 3.25 Hz. The experimental modal shapes are shown in Fig. 7.

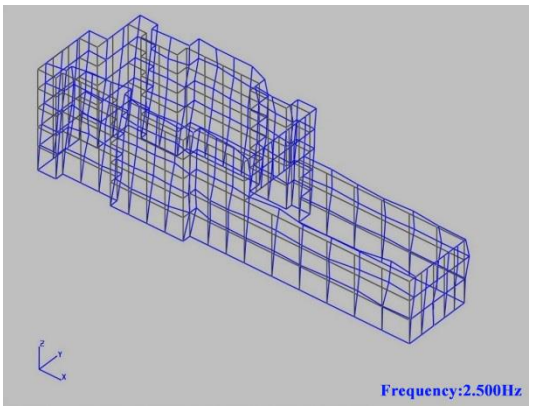

(a) Y- direction first-order bending modal

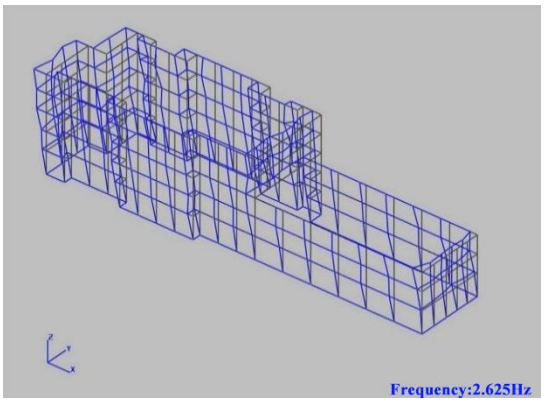

(b) X-direction first-order bending modal

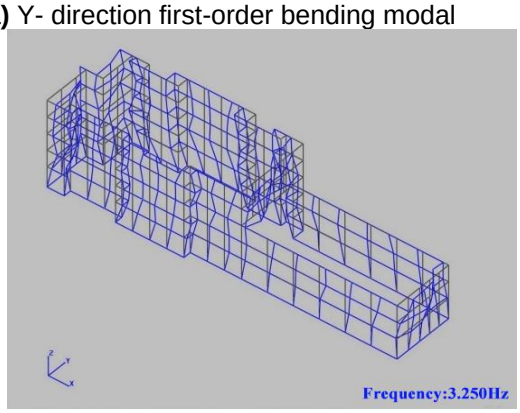

(c) X-direction first-order torsional modal

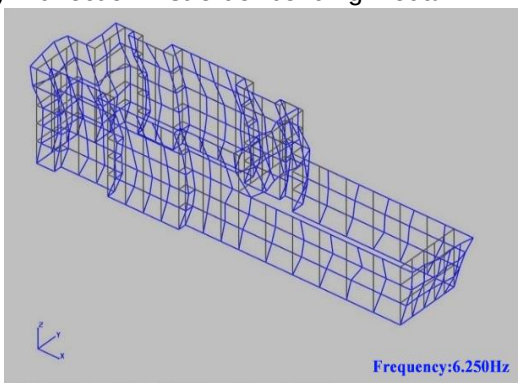

(d) X-direction second-order bending modal

Fig. 7. Experimental modal shapes

Due to the limited energy distribution range of environmental excitation, this experiment did not measure the third and higher-order modal shapes and frequencies of high-rise glulam structures. As can be seen from the frequency parameters in Fig. 7, the first-order bending frequency in the Y-direction is the lowest, and the vibration energy is more likely to concentrate on the first-order bending modal, so the building is more likely to be damaged by the first-order bending in the Y-direction. The first-order torsional frequency measured in this study occurs in the X-direction of the building, which is larger than the first-order torsional frequency in the X and Y directions. This is because the building has three large-volume CLT core tubes, which are approximately evenly distributed in the length direction, increasing the difficulty of building torsional frequency.

It can be seen from the Y-direction first-order bending modal in Fig. 7 (a) that the amplitude of the six-story part in the Y-direction first-order bending is larger than that of the four-story part. Similar to the cantilever beam, this is because the higher the building is, the greater the deviation is more likely to occur under the external dynamic load, and the part away from the fixed end will have a larger amplitude. The inner wall in the middle of the building has a lower amplitude because the entire wall is made of CLT, and the high rigidity in the surface limits the amplitude of the building in the first-order bending modal in the Y-direction.

As for Fig. 7(d), the six-story part shows an obvious X-direction second-order bending modal, while the four-story part only shows an X-direction first-order bending mode, showing the same trend. The second-order bending mode in the middle of the six-story part of the building is the most obvious because there is less arrangement of light

wood shear walls and a large area of glass curtain wall, which has low rigidity in the X-direction and is more prone to large amplitude.

The experimental modal analysis identifies the first-order torsional modal shape in the X-direction, but not in the Y-direction. This phenomenon may be because the X-direction of the building tends to be symmetrical, while the Y-direction torsion shows a difference in height between the top floors. In addition, two of the three CLT cores are on the sixth floor of the building, and the entire CLT wall is also on this part, resulting in a more uneven stiffness distribution in the Y-direction, making torsional vibration patterns complex and difficult to identify.

Comparative Analysis of Calculating Modal and Experimental Modal

From Table 3, it is evident that the results from the calculated modal analysis were generally lower than those from the experimental modal analysis. This discrepancy arises because the complex structure of the test object necessitates an equivalent and simplified approach for the components and nodes in the finite element model. Consequently, this simplification results in a reduced stiffness of the building structure, leading to modal frequency values that are lower than those obtained from field tests. In the torsional modal, the difference is about 13.2%, and in the bending modal, the difference is between 18% and 19%. In the second-order bending modal, due to the difference in height of different parts of the building and the influence of the location of the core cylinder, the Y-direction experimental modal is difficult to identify. The difference in the X-direction second-order bending frequency between the two modal analyses is about 14.6%. Due to the large variety and quantity of components covered by this research object, the equivalence and simplified processing in the calculation of modal analysis will inevitably have a certain impact on the dynamic characteristics analysis. Therefore, the difference between calculation results and test results is acceptable within 20%. According to the results of the calculating modal analysis and the experimental modal analysis, the first three modal categories of the two modal analysis results are consistent. They are first-order bending mode in the Y-direction, first-order bending mode in the X-direction, and first-order torsional mode.

Table 3. Parameter Comparison

Modal Shapes	Calculating Modal (Hz)	Experimental Modal (Hz)	Absolute Error (Relative Error)
X first-order torsional	2.82	3.250	-0.430 (-13.2%)
X first-order bending	2.14	2.625	-0.485 (-18.5%)
X second-order bending	5.34	6.250	-0.910 (-14.6%)
Y first-order bending	2.03	2.500	-0.470 (-18.8%)
Y Second-order bending	5.18	—	—
* Note: "—" means not available			

From the first-order bending mode in the X and Y directions in the calculating modal results, the X-direction first-order bending modal analysis has the characteristics of the first-order bending mode in the Y-direction, and the Y-direction also contains the X-direction partial mode, which is due to the close proximity of the frequencies corresponding to the two modal shapes. The experimental modal analysis is tested separately in the X and Y directions, so the recombination of the first-order bending mode in the two directions is not reflected. The calculating modal analysis and experimental modal analysis are consistent in frequency and vibration mode. The difference in natural frequency is 18.8%,

and the overall frequency difference is within 20%. The experimental modal analysis model has certain reference and feasibility.

The comparison of experimental and calculated modal results indicates that the model simplification method used in this study is feasible and applicable for simulating various types of large timber structures. Additionally, both results demonstrate the significant impact of the CLT core tube on the overall natural frequency of the building. Therefore, incorporating the core tube structure effectively can lower the natural frequency, enhancing the overall comfort and safety of timber building designs.

CONCLUSIONS

1. The model simplification and analysis methods discussed in this article are suitable for modal analysis of this type of building, allowing for the attainment of relatively accurate results. The calculating modal shows that the first-order bending frequencies in the X and Y directions are approximate, and the modal shapes of the two coincide with each other. The six-story part has a greater bending amplitude than the four-story part. The torsional center of the first-order torsional modal is offset to the middle of the six-story part. The natural frequency of buildings occurs in the first-order bending modal in the Y-direction, and buildings are more susceptible to bending failure than torsion.
2. The point-testing method employed in this study effectively captures the modal information of glued-laminated timber structures. The experimental modal shows that the Y-direction first-order bending frequency of the building is the lowest value in the measured data, indicating that the probability of the failure of the building will occur in the form of first-order bending failure. At the same time, the six-story part has a greater amplitude than the four-story part in the first-order bending in the Y-direction. The first-order torsional frequency value of the X-direction is large, and the building is less prone to X-direction torsional damage. The torsional modal in the Y-direction is difficult to identify due to the difference in the height of the top layer of the torsional part of the Y-direction and the uneven stiffness distribution.
3. The calculated modal frequencies align well with the experimental modal frequencies, although the calculated values are generally lower. Specifically, both analyses identify the natural frequencies in the first-order bending mode in the Y-direction, with an error of 18.8% between the two. The smallest error is observed in the first-order torsional mode, at 13.2%. In the X-direction, the frequency errors for the first-order bending and second-order bending modes are approximately 18.5% and 14.6%, respectively. Regarding modal shapes, the distribution of the architectural CLT core along the length significantly affects the modal shape. The first three modal categories from both analyses are consistent. In the first-order bending mode in the Y-direction, the amplitude in the six-story section is greater than that in the four-story section.

ACKNOWLEDGMENTS

Conflict of Interest

The authors have no competing interests to declare that are relevant to this article.

Funding Declaration

This project is funded by the 2024 Forestry Science and Technology Innovation and Extension Project in Jiangsu Province (LYKJ[2024]05).

Date and Code Availability

All relevant data are within the paper.

REFERENCES CITED

ASTM D3737-09 (2009). "Standard practice for establishing allowable properties for structural glued laminated timber (Glulam)," ASTM International, West Conshohocken, PA, USA.

DG/TJ 08-2059 (2009). "Shanghai Urban-Rural Development and Transportation Commission Technical specification for lightweight wooden structure buildings," Shanghai Construction Materials Industry Market Management Station, Shanghai, China.

Gao, Z. Z., Zhang, X., and Wang, Y. (2016). "Measurement of the Poisson's ratio of materials based on the bending mode of the cantilever plate," *BioResources* 11(3), 5703-5721. DOI: 10.15376/biores.11.3.5703-5721

Hayashi, T., and Miyatake, A. (2015). "Recent research and development on sugi (Japanese cedar) structural glued laminated timber," *J. Wood Sci.* 61(4), 337-342. DOI: 10.1007/s10086-015-1475-x

Hafeez, G., Doudak, G., and McClure, G. (2019). "Dynamic characteristics of light-frame wood buildings," *Can. J. Civil Eng.* 46(01), 1-12. DOI: 10.1139/cjce-2017-0266

Jiang, H., Liu, W., and Huang, H. (2022). "Parametric design of developable structure based on Yoshimura origami pattern," *Sustainable Structures* 2(2), article 000019. DOI:10.54113/j.sust.2022.000019

Polastri, A., Izzi, M., and Pozza L. (2019). "Seismic analysis of multi-story timber buildings braced with a CLT core and perimeter shear-walls," *B. Earthq. Eng.* 17, 1009-1028. DOI: 10.1007/s10518-018-0467-9

Quintero, M. A. M., Tam, C. P. T., and Li, H. T. (2022). "Structural analysis of a Guadua bamboo bridge in Colombia," *Sustainable Structures* 2(2), article 000020. DOI: 10.54113/j.sust.2022.000020

Reynolds, T., Harris, R., and Chang, W. (2015). "Ambient vibration tests of a cross-laminated timber building," *Proc. Inst. Civ. Eng-Co.* 168(03), 121-131. DOI: 10.1680/coma.14.00047

Sueyoshi, S. (2008). "Psychoacoustical evaluation of floor-impact sounds from wood-framed structures," *J. Wood Sci.* 54(04), 285-288. DOI: 10.1007/s10086-008-0956-6

Wang, Z., Gu, X. Y., and Mohrmann, S. (2023). "Study on the four-point bending beam method to improve the testing accuracy for the elastic constants of wood, " *Eur. J. Wood Wood Prod.* 81, 1375-1385. DOI: 10.1007/s00107-023-01955-2

Wang, Z., Wang, Z., Wang, B. J., Wang, Y., Liu, B., Rao, X., Wei, P., and Yang. Y. (2014). "Dynamic testing and evaluation of modulus of elasticity (MOE) of SPF dimension lumber," *BioResources* 9(3), 3869-3882. DOI: 10.15376/biores.9.3.3869-3882

Wang, Z., Gao, Z., and Wang, Y. (2015). "A new dynamic testing method for elastic, shear modulus and Poisson's ratio of concrete," *Constr. Build. Mater.* 100, 129-135. DOI: 10.1016/j.conbuildmat.2015.09.060

Wang, Z., Wang, Y., and Cao, Y. (2016). "Measurement of shear modulus of materials based on the torsional mode of cantilever plate," *Constr. Build. Mater.* 124, 1059-1071. DOI: 10.1016/j.conbuildmat.2016.08.104

Wang, Z., Xie, W. B., and Cao, Y. (2018). "Strain method for synchronous dynamic measurement of elastic, shear modulus and Poisson's ratio of wood and wood composites," *Constr. Build. Mater.* 182, 608-619. DOI: 10.1016/j.conbuildmat.2018.06.139

Wang, Z., Xie, W. B., and Lu, Y. (2019). "Dynamic and static testing methods for shear modulus of oriented strand board," *Constr. Build. Mater.* 216, 542-551. DOI: 10.1016/j.conbuildmat.2019.05.004

Wang, Z., Zhang, D., and Wang, Z. (2022). "Research progress on dynamic testing methods of wood shear modulus: A review," *BioResources* 18(1), 2262-2270. DOI: 10.15376/biores.18.1.Wang

Wang, Z., and Ghanem, R. (2023). "Stochastic modeling and statistical calibration with model error and scarce data," *Comput. Method Appl. M.* 416, article ID 116339. DOI: 10.1016/j.cma.2023.116339

Zhang, X., Pan, Y., and Tannert, T. (2021). "The influence of connection stiffness on the dynamic properties and seismic performance of tall cross-laminated timber buildings," *Eng. Struct.* 238, article ID 112261. DOI:10.1016/j.engstruct.2021.112261

Zhu, E. C., Chen, Z., and Chen, Y. (2010). "Experimental and finite element analysis of lateral force resistance performance of light wood structure shear wall," *Journal of Harbin Institute of Technology* 42(10), 1548-1554.

Article submitted: August 7, 2024; Peer review completed: September 21, 2024; Revised version received: September 25, 2024; Accepted: October 18, 2024; Published: October 28, 2024.
DOI: 10.15376/biores.19.4.9616-9630